

Structure and Band Gap Energies of Nano Titanium Dioxide Doped With the Fifth Group Elements

Mohsin E.Al-Dokheily

Chem. Dept. College of Science / University of Thi-Qar mohsinaldokheily@yahoo.co.uk

Abstract

Titanium dioxide powders were synthesized by adding different fifth group elements precursors to titanium (IV) isopropoxide followed by calcination at 500-600 °C. Diffractograms showed the presence of anatase phase except for phosphorus which has amorphous- poly crystalline phase then established a rutile phase among heating above 500°C. Particle size distribution and AFM images indicate the nano dimensions of the studied powders. Particle size distribution varied appreciably in comparison with crystallite size (L) calculated from Scherer formula. Band gap energies calculated from Uv-Vis spectra of thin films deposited on one side of quartz substrate. The band gap energies of TiO_2 –Fifth group elements of this work ranged from 2.83 eV for $N - TiO_2$ to 2.83 eV for $Bi - TiO_2$ with a steady increase according to atomic radii accepts for antimony which deviated from that behavior

Keywords: TiO_2 , Doping, fifth group, Dfractograms, AFM, Band gap

1. Introduction

The large band gap energy E_g 3.2 eV of TiO_2 anatase crystalline phase (Zaleska 2008) has imposed significant limitations on its application particularly in the interior places. Titanium dioxide can utilize only a limited portion of solar radiation, the UV fraction which is at most about 5 percent (Janczarek et al 2007). Titanium dioxide is an n-type semiconductor, and that behavior arises due to oxygen vacancies and creation of Ti^{+3} sites (Pelaes 2012). Rutile phase posses a wider 3d band gap compared to anatase due to localization of Ti 3d states (Di valentine and Pacchioni 2004). In spite of rutile phase has a band gap 3.0 eV compared to 3.2 eV of anatase phase, yet anatase considered to have superior photocatalytic activity because of its larger surface area (Sclafani and Hermann 1996). Extending the absorption of light to the visible range and improving TiO_2 photocatalytic activity require the modification of the band gap.

Implementation of metal and non-metal ions into the lattice of TiO_2 as dopant will bring about a significant lowering of gap energies. Several methods including various types of dopant (Zaleska 2008, Xz and Fa2001, Hsuan-Chung et al 2012), those dopants include d- orbital's transition metals, but more recently non-metals including S, N, C, B, P and F . Also various preparation methods were suggested including chemical vapor deposition (Ding et al 2001) sol gel films (Brinker and Sherar 1990) multilayer deposition (Saciú et al 2009) and pyrolysis of sprays (Raut et al 2009). Anatase titanium dioxide has a tetragonal crystal structure, $D_{4h}^{19} - I4_1/amd, a = b = 3.733 \text{ \AA}, c = 9.370 \text{ \AA}$ while rutile, has a tetragonal crystal structure $D_{4h}^{14} - P4_2/mnm, a = b = 4.594 \text{ \AA}, c = 2.959 \text{ \AA}$. The presence of d-orbital and anionic dopants impair pronounced effects on the titanium dioxide properties (Hanaor and Sorrell 2010). Those effects might lead to reduction of the band gap by creation of new trapping sites which may also control phase transformation to rutile. Cationic dopants may replace Ti of the anatase lattice or may fall on the boundaries of unit cells (Mackenzie 1975). In contrary anionic dopants might replace oxygen of the lattice (Asahi et al 2011). However influence of doping on geometric structure of TiO_2 and virtually optical mechanisms have been calculated by many researchers, (Guo and Du2012) utilized Cambridge Serial Total Energy Package (CASTEP) to study Cu, Ag and Au doped anatase TiO_2 . Density functional theory calculations were used to characterize the doping effects of S substituting for O in anatase TiO_2 Tran et al 2011). The phase stability in doped TiO_2 was carried out using all- electron atomic orbital's methods with local density approximation (Hanaor 2012). The effect of N doping on the surface properties of anatase and rutile TiO_2 were performed using photon - energy range UPS (35 – 110 eV) which is extremely surface sensitive (Batzill et al 2006). Substantial efforts have been subjected toward the commercialization of doped TiO_2 photo catalyses of self cleaning for organic and inorganic compounds in the environment (Fujishima et al 2006).

In this work the TiO_2 band gap was modified by doping with the elements of the fifth group including N, P, As, Sb and Bi using a well established sol- gel method. The structure of prepared powders, particle size and their distribution were identified by XRD and AFM microscopy. The band gap energies were calculated from the UV spectra.

2. Experimental

2.1 Materials

Titanium dioxide anatase (Degussa, purity 99%) used as received without any further treatments. Doped titanium dioxide powders were synthesized as follow: to 10 ml titanium (IV) tetraisopropoxide (Aldrich Purity 97%)

appropriate amount of dopants precursors were added, stirred (Magnetic stirrer LMS100) at 30 °C forming a viscous milky like suspension within 10 minutes ,which is then broke down to a powder after 3 -4 hours of continuous stirring . The powder filtered, dried (Drying oven Fisher Scientific) at 120°C for an hour. The dried powder calcined at 300- 900 °C (Muffle furnace LEF1055, Jlabtech) for an extra hour at each preset temperature .The following precursors were added to titanium (IV) tetraisopropoxide, 5ml of 35% ammonium hydroxide (Aldrich) for $N - TiO_2$, 5 ml of 1M basic solution of As_2O_3 (Fluka) for $As - TiO_2$, 5 ml of 1M of PCl_5 (BDH) for $P - TiO_2$, 5 ml of 1M basic solution of Sb_2O_3 (BDH) for $Sb - TiO_2$ and 5 ml of 1M of $Bi(NO_3)_3$ (Fluka) for $Bi - TiO_2$. Prepared doped TiO_2 powders have different color shades depending as well as on the calcinations temperatures.

2.2 Measurements

2.2.1 XRD

Titanium dioxide and doped titanium dioxide powder XRD were recorded on PAN analytical X'pert PRO MPD using $Cu K\alpha$ as a source for X-ray radiation of 1.5406 \AA from $(0 - 70) 2\theta$.

2.2.2 AFM

Two dimensional and three dimensional particles size and their size distribution were recorded by AA2000 atomic force microscope product of Angstrom Advanced Inc.

2.2.3 Band gap energies

For doped titanium dioxides films were calculated from absorbance spectra recorded on double – beam Uv-Vis spectrophotometer (T90 +) PG instruments. The films were prepared by dipping pre-cleaned quartz substrates vertically in a beaker containing 0.5 g of the synthesized powder suspended in 25 ml deionized water for 30 minutes. The substrate then air dried first and subsequently in an oven at 105 °C for 2 hours. The films deposited on one side of quartz substrates were placed in the sample beam, while uncoated substrate placed in the reference path. The following equation (Mohd et al 2011) was applied

$$A = \frac{h(\nu - E_g)^2}{k\nu} \dots \dots \dots 1$$

Where ν is the frequency in nm, h is the Planks constant and k is a constant. A plot of $(A h \nu)^2$ versus $h\nu$ (eV) gives the band gap E_g value in eV at the intersection of a straight line drawn as a tangent with the x- axis at the absorbance edge.

3. Results and discussions

The fifth group contains two non-metals N and P , as well as three metals As , Sb and Bi . It's well accepted that nitrogen among the best dopants narrowing appreciably the band gap of TiO_2 . According to many theoretical studies nitrogen and phosphorus also might substitute oxygen in titanium dioxide lattice, while other metal members of the group might replace the titanium atom in the lattice. The entire group's elements have $x5^a xP^{a+1}$, $a = 2, x = 2 \text{ to } 6$ outer shell configuration with atomic radii ranging from 75 pm for N to 150 pm for Bi . The group's elements have a correlated opportunity to interact with $O 2s^2 2p^4$ (atomic radius 73 pm) and $Ti 4s^2 3d^2$ (atomic radius 170 pm) of TiO_2 lattice. Therefore the fifth group will present a good model to evaluate the effects of doping. However titanium dioxide provide three possible accommodation sites for dopants, the two substitution site for titanium and oxygen already mentioned above, and the third to interstitial site. The effects of doping include phase transformation from anatase to rutile, and to induce alteration in the electronic structure leads to band gap narrowing facilitating visible light absorption. Both effects were quite evident in forthcoming results.

Figure 1 shows XRD patterns of anatase TiO_2 and different calcined doped TiO_2 . Strong diffraction peaks at $2\theta = 25.3455^\circ (101)$, $37.8298^\circ (103)$, $37.9331^\circ (004)$, $38.6406^\circ (112)$, $48.0772^\circ (200)$, $53.9206^\circ (105)$, $55.1004^\circ (211)$ for anatase TiO_2 . Doping with the fifth group elements by the stated above method brought some major differences into peaks positions characteristic of bare TiO_2 . $2\theta = 27.7930^\circ$ TiO_2 . In $N - TiO_2$ the two small peaks at 37.8298° and 38.6406° appear on the shoulders of the strong peak at 37.9331° of bare TiO_2 are being not clear indicating some structural changes. $P - TiO_2$ Showed a rather different peak position at $2\theta = 29.4227^\circ (110)$, $33.1973^\circ (101)$, $38.3764^\circ (200)$ indicating rutile phase even at early stages of calcinations which was evident at the higher calcinations temperatures. A new peak positions were noticed for As at $2\theta = 28.7235^\circ$, 31.8942° , 32.8073° , and $2\theta = 29.9202^\circ$, 33.4059° , 41.5928° for Sb . Neither $N - TiO_2$ nor $Bi - TiO_2$ showed rutile phase. The ambiguity regarding the effects of the fifth group dopants on the transformation from anatase to rutile may stem from increased density of anion vacancies as in As and Sb dopants as a result from substitution of Ti in anatase lattice⁽¹⁶⁾. Nitrogen as many researchers have agreed might replace oxygen in the anatase lattice efficiently while phosphorus behaved differently. Figures 2 and 3 showed the effect of calcinations from 300 – 900 °C for N and P doped TiO_2 . For $N - TiO_2$ (Fig 2) heating up to 600 °C will bring about a new weak peak at $2\theta = 27.7930^\circ$ referring to emergence of rutile phase. Heating up to 800 °C will turn the powder totally to a

rutile phase which also accompanied by other characteristic rutile peaks at $2\theta = 29.78931^\circ, 36.3422^\circ, 55.5562^\circ$. The diffraction pattern of $P - TiO_2$ (Fig 3) is rather different, at low calcinations temperatures up to 500 the powder is irregular polycrystalline amorphous with low intensity, however the prevailing phase was rutile and it's more pronounced above $600^\circ C$ probably due the formation of well defined crystal dimensions suitable for XRD measurements.

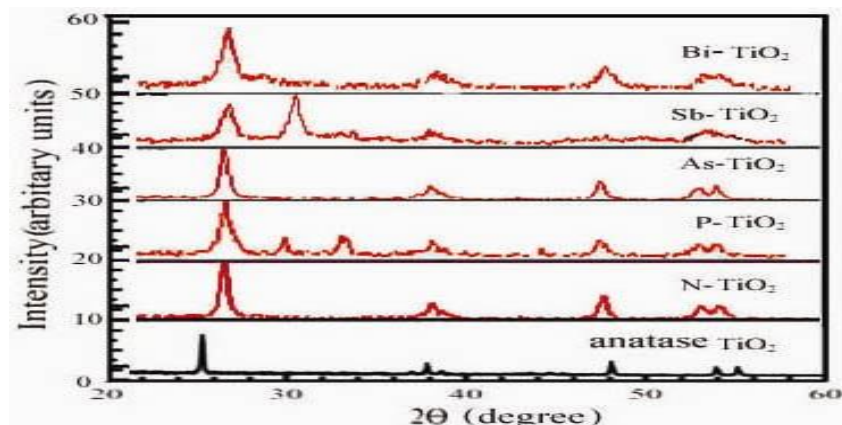


Figure 1: XRD pattern of bare TiO_2 and doped $M - TiO_2$

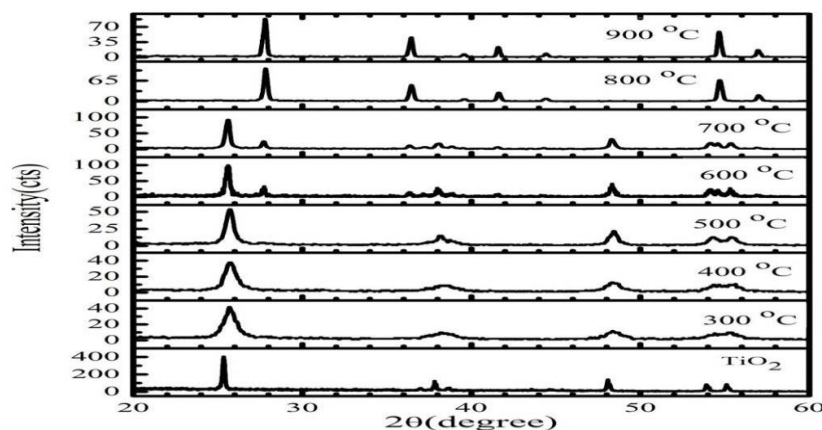


Figure 2: XRD patterns of $N - TiO_2$ calcined at different temperatures

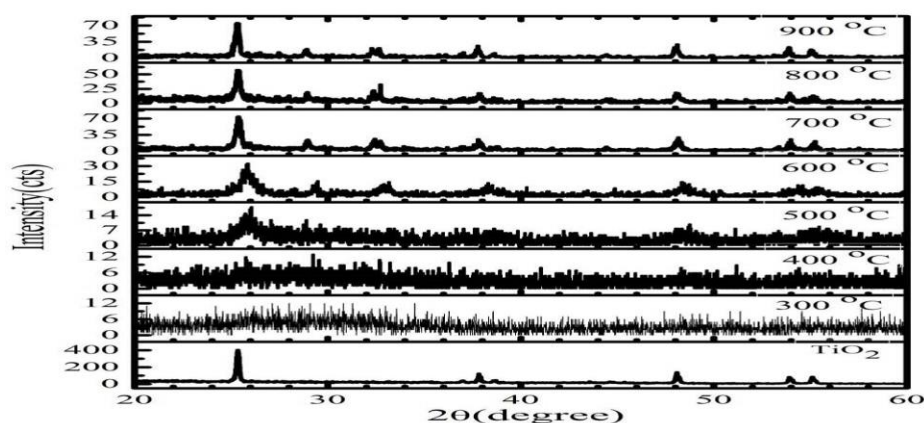


Figure 3: XRD patterns of $P - TiO_2$ calcined at different temperatures

Particle size distribution and AFM images Figures (4, 5, 6, 7, 8 and 9) indicate the nano dimensions of the studied powders. Several measurements have been performed to assure the data. The AFM images showed distinguished regular, smooth and generally round shapes of particles; however particle size distribution varied appreciably in comparison with the crystal size (L) measured by Sherar formula (Monshi et al 2002, Ahmed et al 2014) from XRD diffraction patterns namely for $N - TiO_2$:

$$L = \frac{k\lambda}{\beta \cos \theta} \quad (2)$$

Where k is the Scherrer's constant, in the present calculation a value of 0.94 were adopted. λ Is the wavelength of X-ray source (0.15406 nm), while β is the width of half maximum intensity corresponding to Bragg's angle $FWHM[^\circ 2\theta]$. Results of average particle size (nm) and the average diameters (nm) from AFM measurements as well as the crystallite size L (nm) were listed in table 1.

Table 1: Measured average particle size, their size distribution by AFM and calculated crystallite size L , band gap energies

Code	Particle Size range(nm)	D_{avg} (nm)	L (nm)	Band gap (eV)
anatase TiO_2	60-135	84.19	62.63	3.2
$N - TiO_2$	50-150	95.68	26.03	2.81
$P - TiO_2$	80-180	130.75	59.64	2.83
$As - TiO_2$	30-135	90.98	59.62	2.85
$Sb - TiO_2$	70-140	91.24	49.17	2.84
$Bi - TiO_2$	55-120	78.69	59.62	2.95

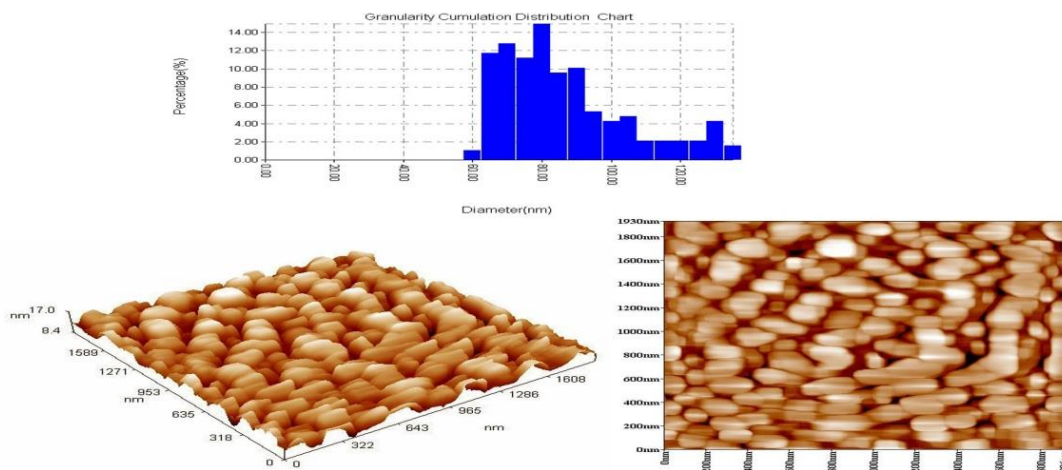


Figure 4: Two and three dimensional AFM images and particle distribution of anatase TiO_2

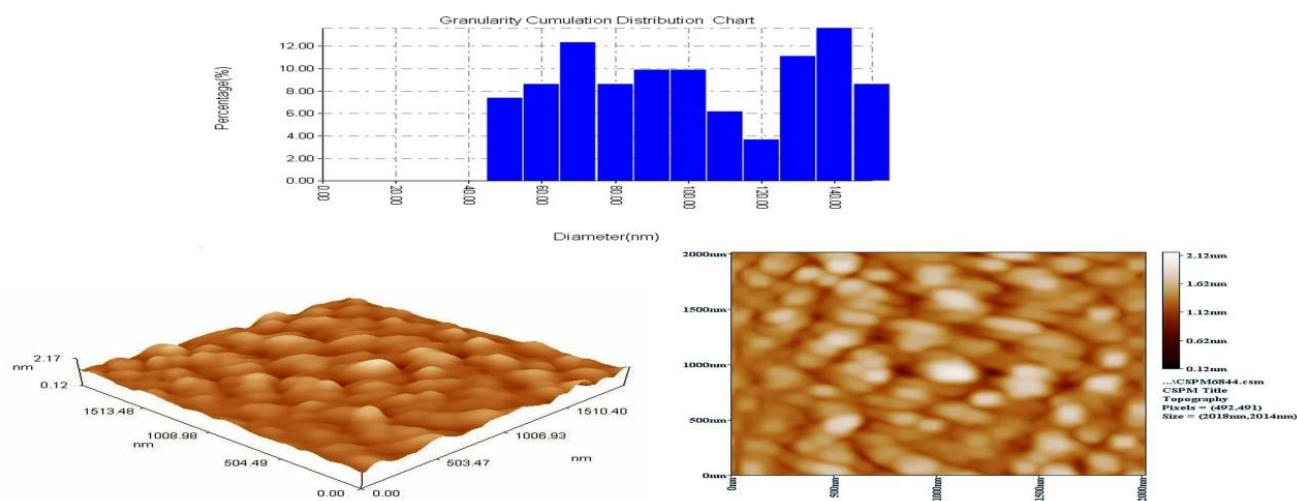


Figure 5: Two and three dimensional AFM images and particle distribution of $N - TiO_2$

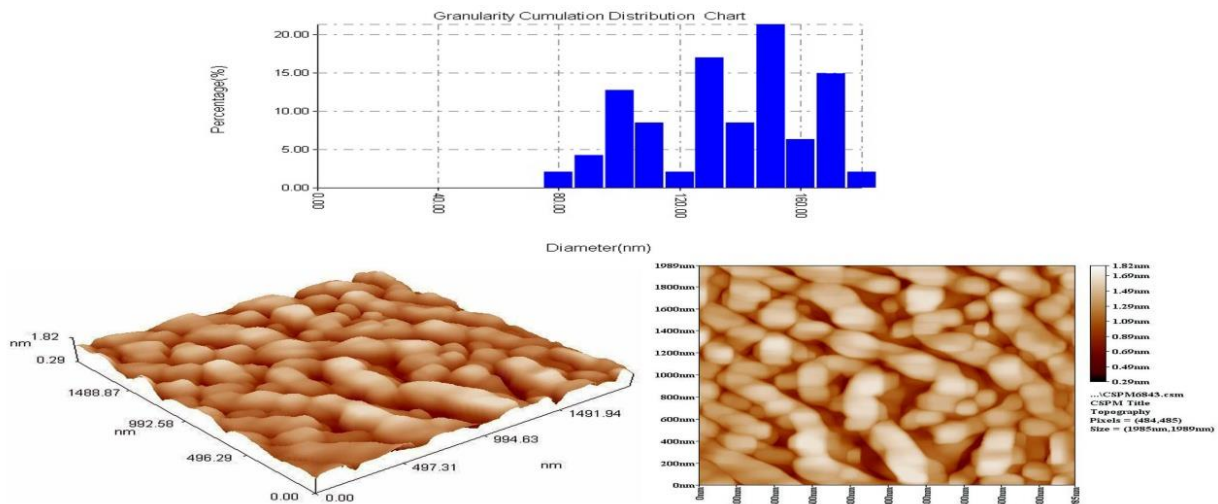


Figure 6: Two and three dimensional AFM images and particle distribution of $P - TiO_2$

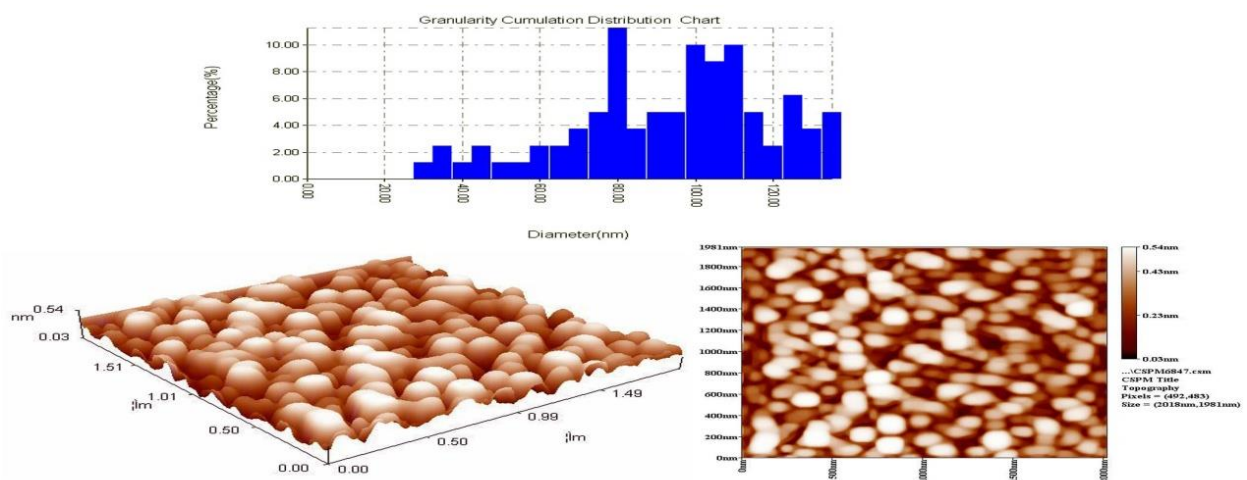


Figure 7: Two and three dimensional AFM images and particle distribution of $As - TiO_2$

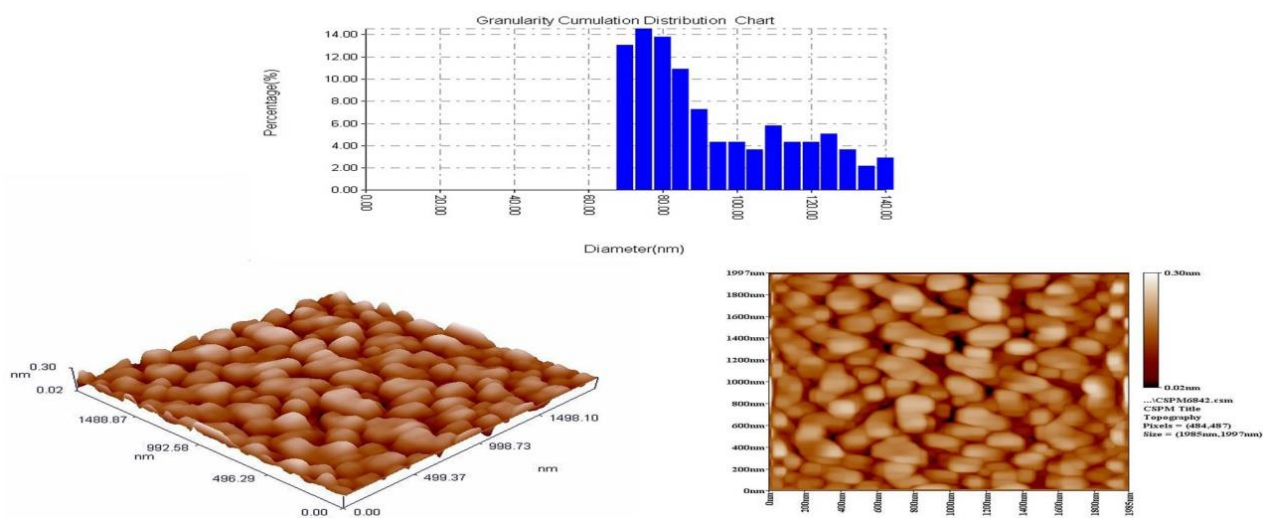


Figure 8: Two and three dimensional AFM images and particle distribution of $Sb - TiO_2$

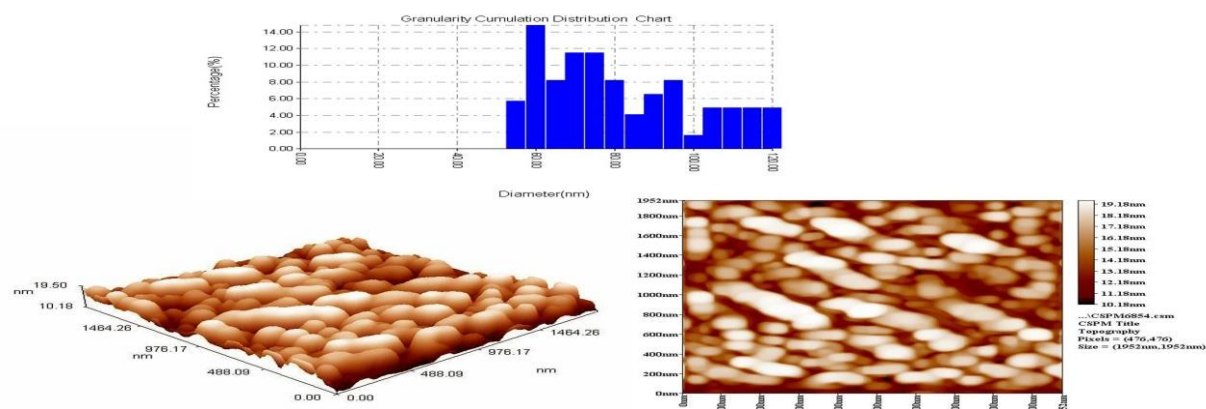


Figure 9: Two and three dimensional AFM images and particle distribution of $Bi - TiO_2$

Figure 11 shows the absorbance spectra of TiO_2 thin films (the curves donated f, g are excluded and they don't belong to the fifth group elements). All of the films were considered transparent above about 460 nm although insignificant absorption tails are still present which probably due to scattered Uv light caused by the thin films them self's (Salah 2013). From figure 11 the extracted absorbance data were plotted as $(Ah\nu)^2$ vs. photon energy $h\nu$ (eV) and presented in figures 12,13,14 and 15. Band gap energies of TiO_2 -Fifth group elements of this work ranged from 2.83 eV for $N - TiO_2$ to 2.95 eV for $Bi - TiO_2$ with a steady increase according to atomic radii accepts for antimony which deviated from that trend. Although many researchers reported rather lower values for $N - TiO_2$ and $P - TiO_2$ powders which may attributed to the measurements of powder instead of films and also to the different experimental conditions such as type of precursors, method of annealing and measurement technique. However doping with the fifth group elements brought about a noticeable correlated narrowing of the band gap energies compared with that of bare TiO_2 . Janezarek etal 2007 suggested a control on the band gap energy by varying nitrogen contents through the control of calcination temperatures rather than varying the nitrogen precursor. Recent study (Hreniak etal 2014) found similar trend for the influence of silver on optical properties of TiO_2 powder.

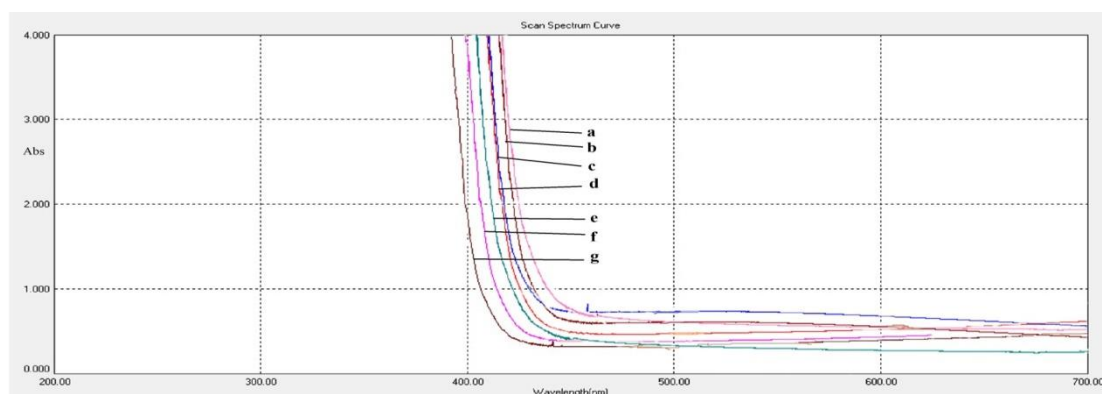


Figure 10: Uv-Vis spectra of doped TiO_2 films with the fifth group elements a) $N - TiO_2$ b) $P - TiO_2$ c) $As - TiO_2$ d) $Sb - TiO_2$ e) $Bi - TiO_2$

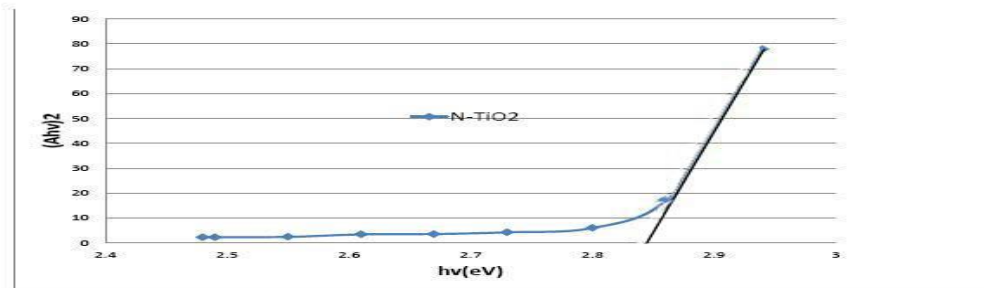


Figure 11: $(\alpha h\nu)^2$ as a function of $h\nu$ for the $N - TiO_2$ Film

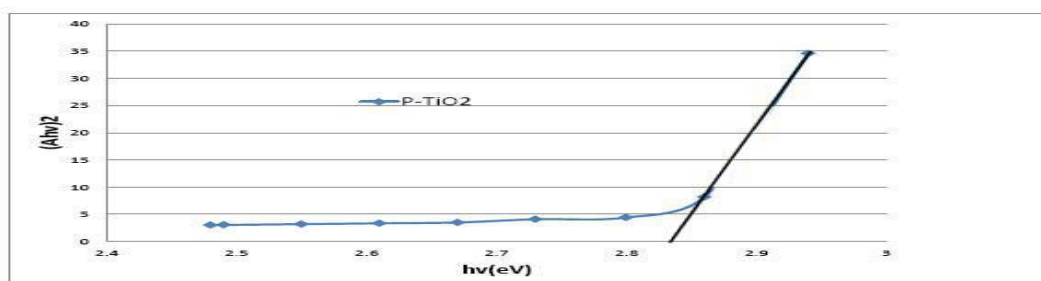


Figure 12: $(\alpha h\nu)^2$ as a function of $h\nu$ for the $P - TiO_2$ Film

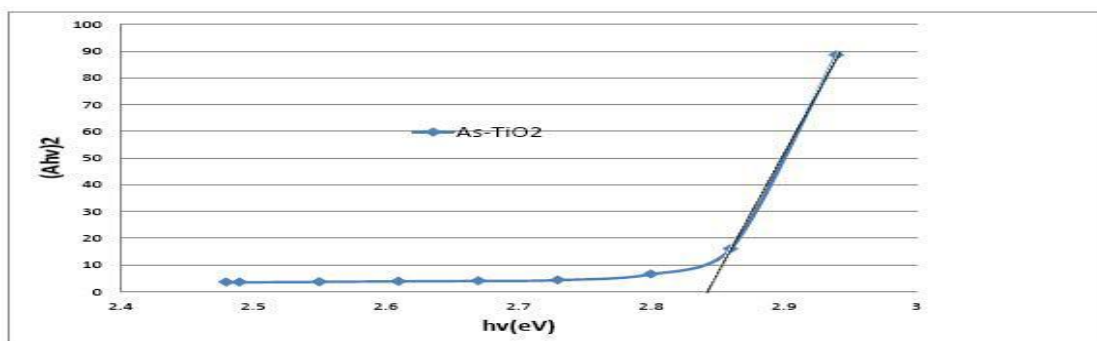


Figure 13: $(\alpha h\nu)^2$ as a function of $h\nu$ for the $As - TiO_2$ Film

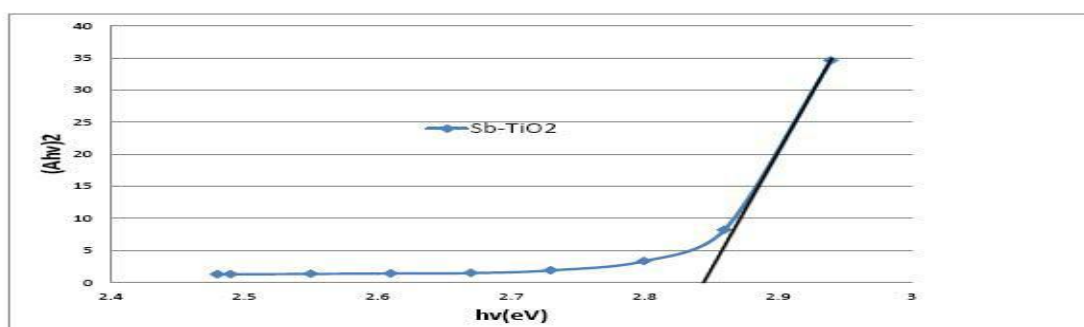


Figure 14: $(\alpha h\nu)^2$ as a function of $h\nu$ for the $Sb - TiO_2$ Film

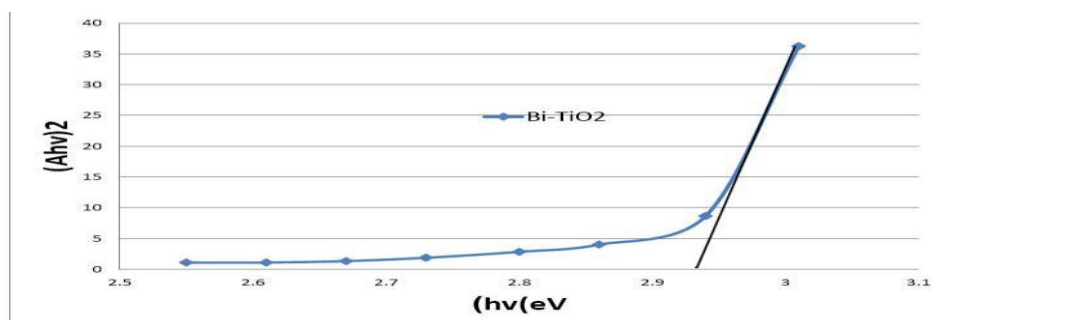


Figure 15: $(\alpha h\nu)^2$ as a function of $h\nu$ for the $\text{Bi} - \text{TiO}_2$ Film

4. Conclusions

Doping of TiO_2 with the fifth group elements brought a noticeable correlated decrease in the band gap from 3.2 eV for bare anatase phase to about 2.85 eV. Synthesized powders have a nano dimensions and almost anatase phase except for phosphorus which has amorphous – mixed phase turned to be rutile above 500 °C. The method of calculating band gap energies gave sharp and easily distinguishable values.

Acknowledgment

This work was supported by the University of Thi-Qar as a part of research and higher studies projects.

References

- Ahmed L.M.; Ivanova I.; Hussein F.H.; and Bahnemann D.W.; 2014; Role of Platinum on TiO_2 in Photocatalytic Methanal Oxidation and Dehydrogenation Reactions; *Int. J. Photo energy*; Article ID 503516
- Asahi R.; Morika W.A.; Hawaki K.; Aoki Y.; 2011; Visible –Light Photo catalysis in doped Titanium Dioxide Oxidation ; *Science* 293,296-271
- Batzill M.; Marels E.; and Dieheld U.; 2006; Influence of Nitrogen Doping on Defect Formation and Surface Properties of TiO_2 Rutile and Anatase; *Phy. Review Lett.* 96, 026103,
- Brinker C.F; and Sherar G.W; 1990; *The Physics and Chemistry of Sol Gel Processing*, Academic press, London
- Di Valentine C; Pacchioni G.; 2004; Origin of the Different Photo activity of N-Doped anatase and Rutile TiO_2 ; *Physical Review B*, 70(8) 085116
- Ding Z.; Hu X, L. Yue P.L.; Lu C.Q.; and Greenfield P.F.; 2001; Synthesis of Anatase TiO_2 Supported on Porous Solids by Chemical Vapor Deposition; *Catalyst Today*, 681.173-182
- Fujishima A.; Zhang X.; and Tryk A.D.; 2004; Heterogeneous Photo catalysis: From Water Photolysis to Application in Environmental Cleanup; *Int. J. Hyd. Energy*, 32(14), 2664-2672,
- Guo M.; and Du j.; 2012; First Principle Study of Electronic Structure and Optical Properties of Cu, Ag and Cu – Doped Anatase TiO_2 ; *arXiv 1203.0701 Chinese National Natural Science Foundation Grant No. 11175128*.
- Hanaor D. A.H.; Assad M.H.N.; Yu S.A.; and Sorrell C.; 2012; AB Initio Study of Phase Stability in Doped TiO_2 ; *Com. Mechanics*, 50(2), 185-184
- Hanaor D.A.H.; and Sorrell C.C.; 2010; Review of the anatase to rutile phase transformation; *J. Mater. Sci.* 46:855–874
- Hreniak A.; Sikora A.; and Iwan A.; 2014; Influence of Amount of Silver on Structural and Optical Properties of TiO_2 Powder Obtained by Sol- Gel Method; *Int. J. of Mater. Chem*, 4(2), 15-2
- Hsuan-Chung Wu; Sheng-Hong Li; Syuan-Wei Lin; 2012; Effect of Fe Concentration on Fe – Doped TiO_2 From GGA + U Calculations ; *Int. J. Photo energy*; Article ID frame, 823498, 6 pages
- Janczarek M.; Kisch H.; Hupka J.; 2007; Photoelectrochemical Characterization of Nitrogen modified TiO_2 ; *Photochemical Problems of Mineral Processing*; 41,159-166
- Mackenzie KJD; 1975; Calcination of Titania v. Kinetics and Mechanism of the Anatase – Rutile Transformation in the Presence of Additives; *Transactions and Journal of The British Academic Society* 74, 77-84
- Mohd A.K.; Rosli Y.; and Min H.; 2011; Uv-Visible Studies of Chemical Bath Deposited NiSe Thin Films; *Int. J. Chem. Res.*, 3(1), 21-26
- Monshi A.; Foroughi M.; and Monshi M.; 2002; Modified Scherer Equation to Estimate More Accurately Nano-Crystallite Size Using XRD; *World J. Nano Sci. Eng.*, 2,154-160
- Pelaeza M.; NolanbN.T.; Pillaib S.C.; Seeryc M.K.; Falarasd P.; Kontosd A.G.; Dunlope P.S.M.; Hamiltone . J.W; Byrnee A. J., O'Sheaf K.; H. Entezarig M.H.; Dionysioua,D.D. ; 2012; A review on the visible light active titanium dioxide photocatalysts for environmental applications; *Appl. Catalysis B: Environ.* 125, (21), 331–349

- Raut N.C; Mathews T.; Sunder S.F ; Sairam T.N; Dash S; Tayqi A.K;2009; Structural and Morphological Characterization of TiO_2 Thin Films Synthesized by Spray Pyrolysis Technique; J. Nano Science Technol,9(4) ,5298-302
- Saciu R.C.; Inderea E. ;2009; Silipas T.D.; Dreve S.I. Rosa M.C.; Popescu V.; Popescu G.; and Nascu H.I.; TiO_2 Thin Films Prepared by Sol- Gel Method; *J.Phy. Conference Series 182*, 012080
- Salah A. F.; 2013; Structural and Morphological Studies of NiO Thin Films Prepared by Rapid Thermal Oxidation Method; *Int.J. Appl. Annov.Eng&mang*, 2(1), 16-21
- Sclafani A.; and Herrmann J.M.; 1996; Comparison of Photo electronic and Photocatalytic Activities of Various Anatase and Rutile Forms of Titania; *J.Phy.Chem.*'100.13655-13661,
- Tran F.; Liu C.; Zhao W. ; Wang X.; Wang Z.; and Yuc J.;2011; Cationic S- Doped Anatase TiO_2 a DFT Study ; *J. Com. Sci. Eng.* 1,33-41
- XZ L.;FA L.;2001; Study of $Au/Au^{+3} - TiO_2$ Photo catalysis Towards Visible Photoxidation for Water and Waste Water Treatment; *Environ .Sci. Technol.* 35,2281- 2387
- Zaleska A.; 2008; Doped TiO_2 : A Review; *Recent Patents of Engineering*: 2,157,157-164

The IISTE is a pioneer in the Open-Access hosting service and academic event management. The aim of the firm is Accelerating Global Knowledge Sharing.

More information about the firm can be found on the homepage:

<http://www.iiste.org>

CALL FOR JOURNAL PAPERS

There are more than 30 peer-reviewed academic journals hosted under the hosting platform.

Prospective authors of journals can find the submission instruction on the following page: <http://www.iiste.org/journals/> All the journals articles are available online to the readers all over the world without financial, legal, or technical barriers other than those inseparable from gaining access to the internet itself. Paper version of the journals is also available upon request of readers and authors.

MORE RESOURCES

Book publication information: <http://www.iiste.org/book/>

IISTE Knowledge Sharing Partners

EBSCO, Index Copernicus, Ulrich's Periodicals Directory, JournalTOCS, PKP Open Archives Harvester, Bielefeld Academic Search Engine, Elektronische Zeitschriftenbibliothek EZB, Open J-Gate, OCLC WorldCat, Universe Digital Library, NewJour, Google Scholar

